

OPEN ACCESS

\*CORRESPONDENCE

Pshtiwan O.Zaid,

[Pshtiwan.zaid@su.edu.krd](mailto:Pshtiwan.zaid@su.edu.krd)

RECEIVED :20 /05/ 2023

ACCEPTED:06/01/ 2024

PUBLISHED:30/ 06/ 2024

KEY WORDS:

Rectangular Sharp crested weir, Experimental work, Water surface profile, Ansys-Fluent.

# The Validation of Rectangular Sharp Crested Weir Flow using ANSYS – FLUENT

Bruska S. Mamand<sup>1</sup>, Pshtiwan O. Zaid<sup>2\*</sup>

<sup>1,2</sup>Department of Water Resources Engineering, College of Engineering, Salahaddin University-Erbil, Erbil, Kurdistan Region, Iraq.

A weir is a structure consisting of an obstruction such as a dam that built across the open channel to change its flow characteristics. In the present study, a total 12 experiments were done in the laboratory of civil engineering department inside an open channel with 20 cm width and installing full width rectangular sharp crested weirs. Then the numerical runs were validated with experimental findings and additional runs were done. The implementation of Numerical Methods A volume of fluid (VOF) model was created for the situation when water and air are in direct contact with one another. Three distinct k-epsilon turbulence models were examined [standard, RNG, and realizable]. According to mass balance data, the greatest error in experimental measurements between the main channel's input and outlet discharges does not exceed 9.542%. Furthermore, average percentage of error between numerical and experimental outlet discharges for standard, RNG and realizable k- epsilon method was 7.235, 5.489 and 7.301 respectively. Cd increased with increasing the ratio of (H1/P). The water surface will be stable along 2 m of upstream channel length upstream of the sharp crested weir, and the longitudinal water levels will decrease slightly over the weir with a curved profile, as determined experimentally and numerically.

## 1. Introduction

In general, a sharp crested weir is a simple type of overflow dam. In the lab, it is used as a structure for measuring the flow rate. It can be used in many areas of everyday life, like industry and water systems.

The most recent efforts to represent two-phase flow with the fluent code are presented in the aforementioned literature review (Pavel and Fakultastrojni, 2008). In addition to an explicit volume of fluid (VOF) model, other critical simulation parameters were integrated, including the pressure velocity relation, the discretization scheme body force weighted for pressure, and the second order upwind for momentum. The k-turbulence model was used by (Ramamurthy et al., 2009) to predict the distributions of pressure heads, velocities, and water surface profiles that characterize a flow. The flow behavior of a sharp-crested weir in a rectangular open channel may be predicted using the well-known k-turbulence model. The free surface's form may be determined using the volume of fluid (VOF) method. Over a rectangular sharp crested weir, flow and a method for estimating the discharge coefficient were examined in (Mahtabi, G. and Arvanaghi, H., 2018). The importance of investigating velocity vectors and pressure patterns across rectangular sharp-crested weirs in three-dimensional space has been underlined. (Hadi and Navid, 2013) used both experimental and numerical data to investigate the impact of the weir height, the Froude number, and the Reynolds number on the weir discharge coefficient. The free surface profile of a rectangular broad crested weir was calculated by (Hosseini and Hooman, 2013) using a Computational Fluid Dynamics (CFD) model and a laboratory model. Triangular labyrinth weirs, a non-linear weir used to control free flow over low-width weirs, have been studied (Mahmoud Reza et al., 2015). (Ghorban and Hadi, 2018) looked at free-flow experiments with sharp-crested weirs. The flow over a steep crested weir was simulated using a three-dimensional numerical model (Hamid et al., 2020). The velocity and surface properties of the simulated data were compared to the experimental data. The investigation used three distinct k-turbulence models based on the

volume of fraction (VOF). (Zaid, P.O., 2022) used ANSYS-FLUENT, based on Finite Volume Method combined with Volume of Fluid to capture free-surface flow properties is to model the hydraulics of skimming flow through uniform stepped spillways with moderate chute slope  $26^\circ$  in 45 different cases to find the performance of flow over stepped spillway. (Zaid, P.O. and Abo, A.A, 2023) worked on CFD method to find the location of inception point on stepped spillway for different size, shape, and angle of steps. (Malekzadeh et al., 2022) demonstrate numerical simulation with ANSYS FLUENT software. There are 432 simulations in all, with 4 upstream slopes, 4 downstream slopes, 3 weir heights, 3 upstream heads ( $h_1$ ), and 3 weir crest lengths. They discovered that the slope of the downstream face had no influence on Cd. Cd rises for 0.1  $H_1/w$  0.4 by reducing the upstream slope, where  $H_1$  is the water head on the weir crest and  $w$  is the length of the crest. In addition, over the same range, reducing the height of the weir ( $p$ ) increases the Cd. For 0.16  $H_1/p$  2, the Cd increases as the length of the crest diminishes. Multivariable regression equations for estimating Cd are provided by comparing numerical simulation findings to practical data. (Singh and Sen, 2023) investigates the influence of a short-crested trapezoidal weir's downstream slope on its flow hydraulics and conveyance capabilities. Aside from channeling water to a canal, irrigation barrages and weirs aid in monitoring river discharge, which is a function of upstream and downstream water levels. For huge discharges during floods, the gates of a barrage are opened to allow for an unregulated flow that may be free or submerged depending on the downstream water level. Although previous research on uncontrolled flows acknowledged the effect of a weir's upstream slope on the coefficient of discharge, this study proves that it is also influenced by the downstream slope of a weir.

## 2. THEORITICAL CONSIDERATIONS:

### 2.1 Discharge Equation and Dimensional Analysis

By assuming a rectangular weir with a length ( $L$ ) equal to the width ( $B$ ) of a rectangular channel (i.e.,  $L = B$ ), the discharge equation for free flow

over a sharp-crested weir can be found as a function of the depth of flow upstream of the weir, as measured above the weir crest ( $H_1$ ):

$$Q = \frac{2}{3} C_d \sqrt{2g} B H_1^{3/2} \dots\dots\dots (1)$$

Where  $C_d$  is coefficient of discharge.

The Buckingham's  $\pi$ - theorem was used for assessment of the main variables controlled the flow passed on full width rectangular sharp-crested weir. As shown in Figure 1, the open channel width ( $B$ ), depth of water above the sharp crested weir ( $H_1$ ), weir height ( $P$ ) and the characteristics of the fluid includes a mass density ( $\rho$ ) are effects on the discharge coefficient of flow passed over the weir.

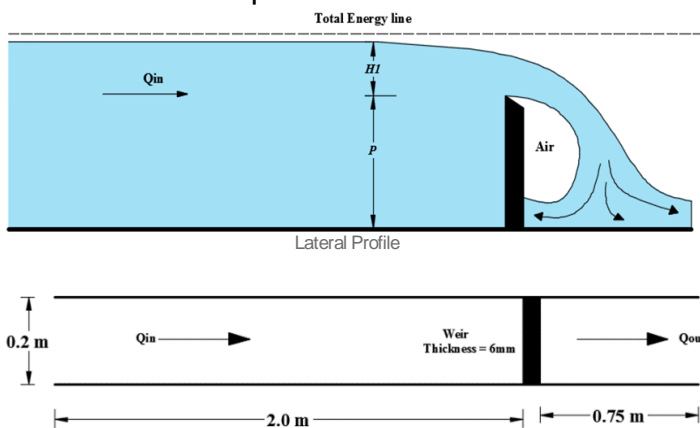


Figure1: Position of the weir inside rectangular flume

The basic expressions for the dimensional analysis are as follows:

$$Q_{in} = f (V_1, B, H_1, P, \rho, g) \dots\dots\dots (2)$$

After performing the dimensional analysis, the following relations are obtained:

$$C_d = f \left( \frac{B}{P}, \frac{H_1}{P} \right) \dots\dots\dots (3)$$

In ideal fluid flow  $C_d = f(H_1/P)$  and the variation of  $C_d$  for rectangular sharp crested weirs is given by the well-known Rehbock formula ( $C_d = 0.611 + 0.08 \frac{H_1}{P}$ ), which is valid for  $H_1/P \leq 5$

**2.2 Numerical Theories**

This article introduced the fundamental concepts and practical applications of numerical modeling for flow over a rectangular sharp-crested weir. Computational fluid dynamics (CFD) involved the use of numerical techniques to solve mathematical equations describing fluid flow. Numerical modeling used methods like the finite

volume approach to solve partial differential equations using a variety of computer algorithms. Using the FLUENT programme interfaced on ANSYS V.14, (Zaid, P.O. and Abo, A.A, 2023), we analyzed experimental models of varying weir heights to determine how to achieve a broad spectrum of flow characteristics with sharp crested weirs. Navier-Stokes is the name of the governing equation for fluid motion. As non-linear differential equations, these equations have several possible analytical solutions. (Desai and Patil, 2015) give the following three-dimensional variant of the Navier-Stokes equation for an unstable viscous in the x-direction:

$$\frac{\partial u}{\partial t} + \frac{1}{V_F} (uA_x \frac{\partial u}{\partial x} + vA_y \frac{\partial u}{\partial y} + wA_z \frac{\partial u}{\partial z}) = -\frac{1}{\rho} \frac{\partial p}{\partial x} + G_x + f_x \dots\dots\dots (4)$$

It is supplemented by the mass conservation equation:

$$\frac{\partial u}{\partial x} A_x + \frac{\partial v}{\partial y} A_y + \frac{\partial w}{\partial z} A_z = 0 \dots\dots\dots (5)$$

The momentum equation is:

$$\frac{\partial}{\partial t} (\rho U_i) + \frac{\partial}{\partial x_j} (\rho U_i U_j) = -\frac{\partial P}{\partial x_i} + \frac{\partial}{\partial x_i} \left[ \mu \left( \frac{\partial U_i}{\partial x_j} + \frac{\partial U_j}{\partial x_i} \right) \right] + \rho g_i + \bar{F} \dots\dots\dots (6)$$

Where:  $P$  = pressure,  $g$  is acceleration due to gravity.  $\mu = \mu_0 + \mu_t$   
 $\mu_0$  is viscosity of fluid,  $\mu_t$  = turbulence viscosity and  $F'$  is the body force.

**2.3 Multi-Phase and Turbulence Model**

Volume of fluid (VOF) surface tracking method. The VOF model was used to track the liquid-gas (water and air) interphase of two or more immiscible fluids (i.e., able to mix) (Zaid, P.O. and Abo, A.A, 2023). FLUENT offers multiple turbulence models to solve multiphase systems with distinct transport equations. This research employed a different k-e model:

$$\frac{\partial(\rho k)}{\partial t} + \frac{\partial(\rho k u_i)}{\partial x_i} = \frac{\partial}{\partial x_j} \left[ \left( \mu + \frac{\mu_t}{\sigma_k} \right) \frac{\partial k}{\partial x_j} \right] + G_k + G_b - \rho \varepsilon - Y_M \dots\dots\dots (7)$$

$$\frac{\partial(\rho \varepsilon)}{\partial t} + \frac{\partial(\rho \varepsilon u_i)}{\partial x_i} = \frac{\partial}{\partial x_i} \left[ \left( \mu + \frac{\mu_t}{\sigma_\varepsilon} \right) \frac{\partial \varepsilon}{\partial x_j} \right] + C_{1\varepsilon} \frac{\varepsilon}{k} (G_k + C_{3\varepsilon} G_b) - C_{2\varepsilon} \rho \frac{\varepsilon^2}{k} \dots\dots\dots (8)$$

The eddy viscosity is completed by combining  $k$  and  $\varepsilon$  as follows:

$$\mu_t = \rho C_\mu \frac{k^2}{\varepsilon} \dots \dots \dots (9)$$

**2.4 Experimental Setup and Flowrate Measurements**

This investigation made use of the fluid mechanics laboratory at the civil engineering department of a university. Full-width rectangular sharp crested weirs were used in the experiments, with the heights ( $P= 0.1$  and  $0.12$  m). The main channel, which is  $0.2$  m wide and  $0.4$  m deep, features a sharp crested weir. Before the weir, the canal is  $2$  meters in length, whereas beyond it, it is just  $0.75$  meters. Perspex plastic with a thickness of  $0.006$  m was used to make the weirs. The experimental setup was shown in **figure 2**.

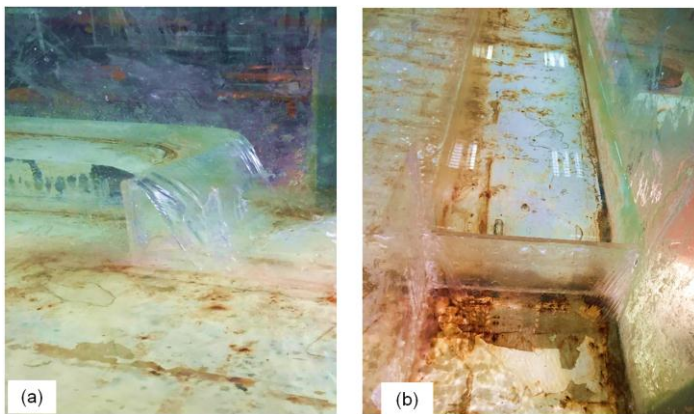


Figure 2. Open channel and sharp crested weir. a) Side view, b) Top view.

Table 2 1: different runs for different P and flows

No.	$Q_{in}$ (L/s)	P (m)
1	3.085	0.1
2	6.027	0.1
3	9.08	0.1
4	12.05	0.1
5	15.07	0.1
6	18.11	0.1
7	21.12	0.1
8	9	0.12
9	12	0.12
10	15	0.12
11	18	0.12
12	21	0.12

Downstream of the main tank, a v-notch weir was built to quantify  $Q_{in}$ , or the total discharge into the main canal. The water depth at upstream of the weir was measured ( $H_v$ ) and the total channel discharge can be calculated according to below

equation by (Sargison, J.E. and Percy, A., 2009) as:

$$Q_{in} = 0.0194 H_v^{2.4015} \dots \dots \dots (10)$$

The discharge at the downstream of the main channel ( $Q_{out}$ ) can be determined by equation (1) as aforementioned earlier.

**3. STEPWISE OF ANSYS FLUENT**

**3.1 Creating Geometry**

The FLUENT code, which interfaced with the ANSYS (14.0) program, was used to build a variety of different shapes of sharp crested weirs, which are seen in **figure 3**

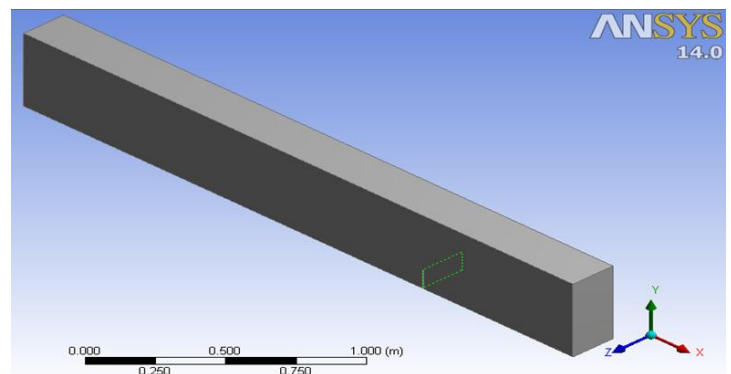


Figure 3. Geometry of an open channel and full width weir.

**3.2 Defining Mesh**

The present investigation employs an automated mesh approach to compute mesh grids throughout a solid domain, as seen in Figure 4. The mesh size used in this study was  $0.0075$  m, which was tiny enough to guarantee that flow characteristics were dispersed throughout all fields. Findings compared to previous experimental information. The "Fixed" setting in the advanced sizing menu was activated, and high smoothness was chosen for the size.

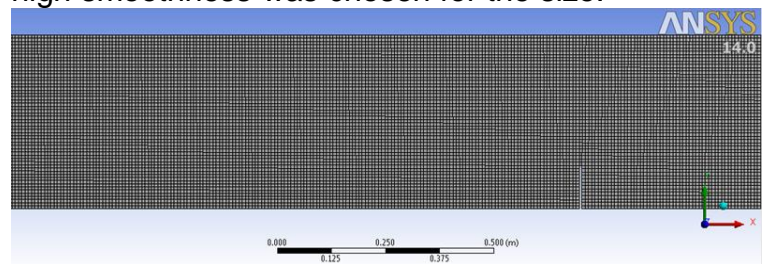


Figure 4. Mesh defining of rectangular channel and sharp crested weir.

**3.3 Setting Boundary Conditions**

Figure5 illustrates and clarifies the boundary

conditions at several locations.

- The inlet section, where water only flows into the channel, was used to establish the inlet border, and the inlet water depth and inlet velocity magnitude were determined experimentally. Place it at the domain's intake, where the air phase first entered at a total pressure of zero. Unit volume fractions of air and water were used to get the fluid values.
- The downstream regions where fluid exits the domain have an outlet border established. The volume portion of the return flow as a percentage was also input.
- The ambient limit was set at the channel's top opening. It was necessary to have air pressure of zero atmospheres and a volume fraction of one unit return flow.
- The breadth of the bottom, the sides of the channel, and the heights of the weirs were all designed to be immovable walls that prevent flow, and the walls are smooth and no slippery.

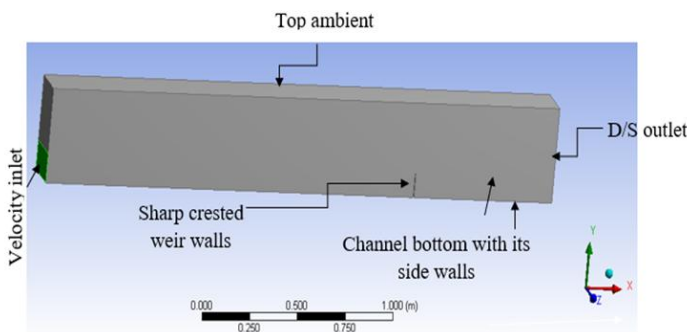


Figure 5. Locations of boundary conditions.

The variables  $k$  and  $\epsilon$  were used to define the inlet and outlet borders, and the body force weighted for pressure approach and the second order upwind technique were utilized to solve the finite volume equations for the mass, momentum, and turbulence models, respectively.

#### 4. RESULTS AND DISCUSSION:

##### 4.1 Discharge Calculation and Mass Balance

The flow flowing over the steep crested weir ( $Q_{out}$ ) is reliable since mass balancing studies reveal that the highest error in the experimental measurements between the inflow and outflow discharges of the main channel does not exceed 9.542%. The roughness of the channel bed and the precision of the experimental point gauge

both contribute to this inaccuracy. As can be seen in Figure 6, the mass balance between the inflow and outflow discharges was accurately predicted by the numerical models used to compute the flow parameters across the weir.

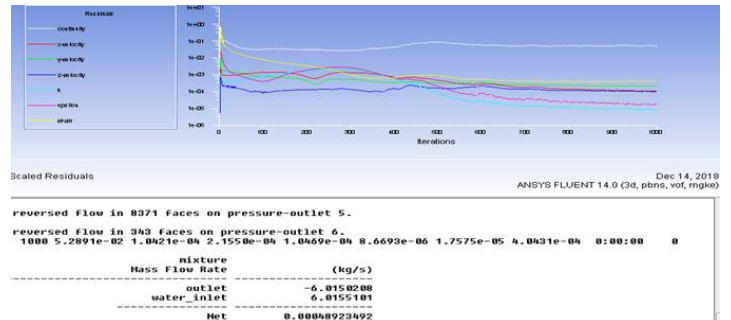


Figure 6. Residual window and mass balance results.

##### 4.2 Effect of Turbulence Models

Different turbulence models' numerical solutions were verified for accuracy. Here, we provide the results of numerical experiments performed on three different k-epsilon turbulence models (standard, random number generator, and realizable). Seven distinct experimental discharges were simulated. Figure 7 shows the relationship between inlet and outlet channel discharges for the three k-e approaches that were examined. These techniques verify the accuracy of the numerical answers by comparing them to real-world experiments. The proportion of the difference between upstream and downstream discharge in the main channel is modest enough to be ignored.

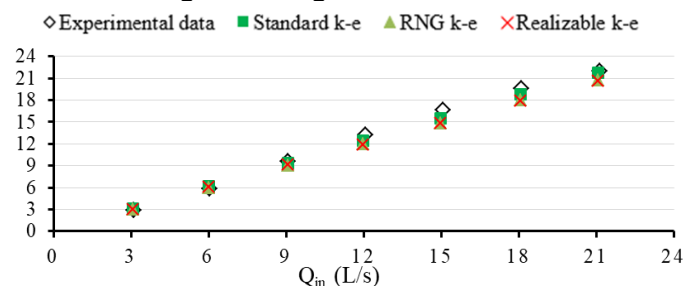


Figure 7. Comparison of k-epsilon turbulence models with experimental data for  $P=10$  cm.

Figure 8 further shows that the average percent error between numerical and experimental outlet discharges was 7.235 for the conventional technique, 5.489 for the RNG method, and 7.301 for the realizable k-epsilon method. This finding explains why the RNG k-epsilon model, the best model for solving flow in the channel passed over the steep crested weir, has such a tiny average

percent of error. When compared to other runs, the standard and realizable k-e technique was only slightly off from one another, with the biggest % error.

Table 4 1:Error comparison of two types of k-epsilon turbulence models

RNG k-e			Standard k-e		
Qin (L/s)	Qout (L/s)	% error	Qin(L/s)	Qout (L/s)	% error
3.075	3.158	11.048	3.080	3.041	6.909
5.996	6.227	6.911	6.016	6.015	3.280
9.064	9.371	2.036	9.064	9.048	5.419
11.979	12.408	6.369	11.979	11.942	9.885
14.959	15.526	6.825	14.959	14.882	10.687
18.076	18.788	4.399	18.075	17.962	8.600
21.081	21.799	0.832	21.081	20.692	5.867

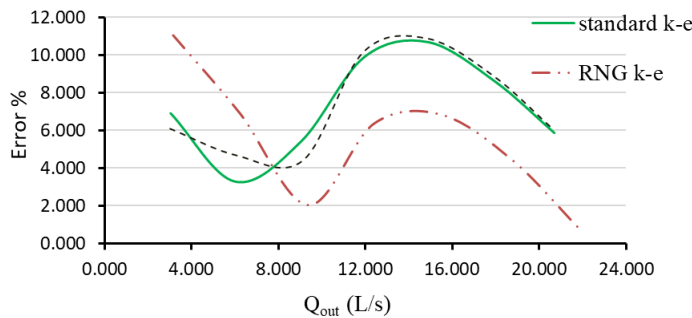


Figure 8. Error comparison of two types of k-epsilon turbulence models

### 4.3 Water Surface Profile

The longitudinal profile of the water's surface is presented here for a subcritical flow regime within the main channel. The experiments are crucial for determining the numerical outcomes, as was previously described. Water volume fraction contours were drawn for numerical studies, as illustrated in Figure 9. The depth readings were obtained near the middle of the main channel. In which a polyline representing water levels was drawn using contours of water volume fraction projected on a rectangle plane. Three different k- e turbulence models (Standard, RNG, and Realizable) was tested to insure the suitability of each models.

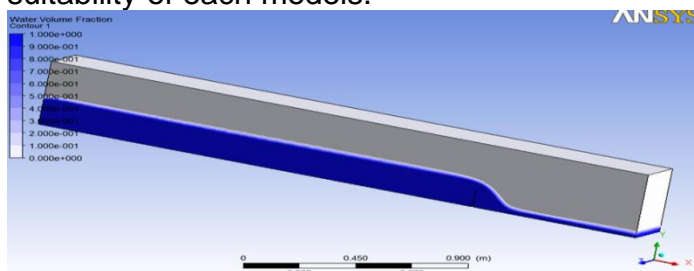


Figure 9. 3D view of water volume fraction.

Discharge values were observed to vary over a weir of varying heights. Several k-e turbulence models with varying run discharges were shown in a series of images for visual comparison. From Figure 10, the x-axis of the graph represents the distance from the inlet channel boundary and y-axis represents the water height from the bottom of the channel. The water surface will be stable for 2 meters upstream of the sharp crested weir, and then the longitudinal water levels will decrease slightly over the weir with a curved top, as shown in the detailed water surface profile both upstream and downstream.

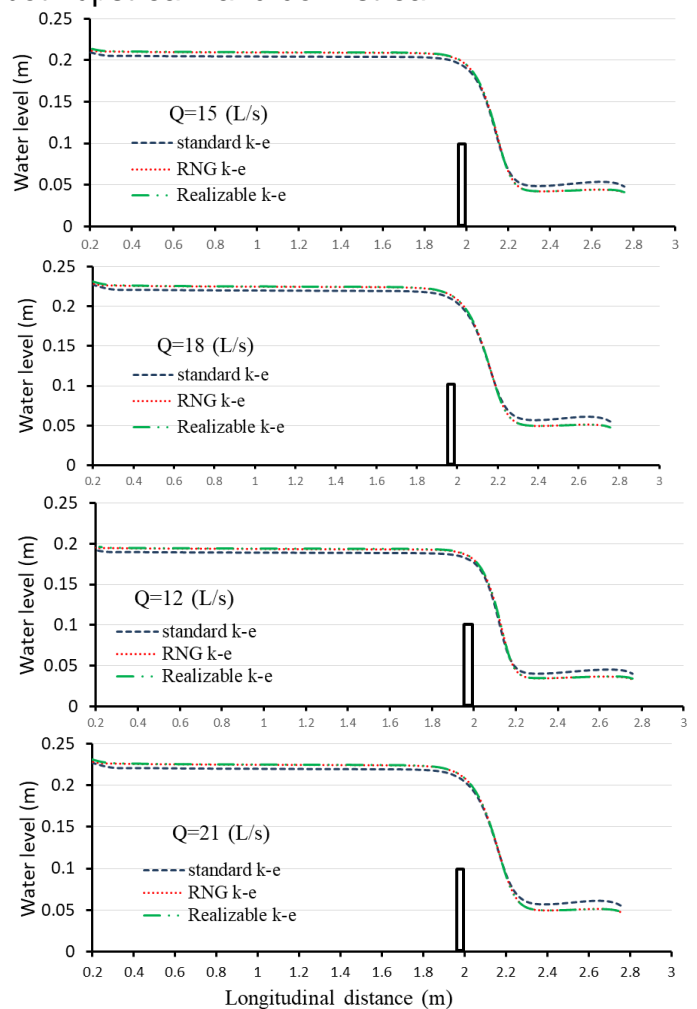


Figure 9. 3D view of water volume fraction.

### 4.4 Effect of Dimensionless Parameters on Discharge Coefficient:

The most effective dimensionless parameter that affected on the discharge coefficient ( $C_d$ ) is the ratio of height of water above weir to the weir

height ( $H_1/P$ ).

Figure 11.a, shows results of experimental and numerical  $C_d$  versus  $H_1/P$  for weir height is 0.1 m.  $C_d$  increased with increasing  $H_1/P$ . in this study, For values of  $H_1/P$  greater than 0.3,  $C_d$  approximately reached the fixed value of 0.62 to 0.72. In other words, the variation of  $H_1/P$  had a great effect on the discharge coefficient when  $H_1/P > 0.3$ . Almost little difference could be seen between the numerical and experimental results. While there were some discrepancies between the experimental and numerical results, they were so minor as to be disregarded. These results indicate that fluent software can simulate the flow over the weir very well. Similarly, Figure 11.b, shows the variation of  $C_d$  for weir height is 0.12 m.  $C_d$  increased with increasing  $H_1/P$  and also the numerical results were very close to experimental data.

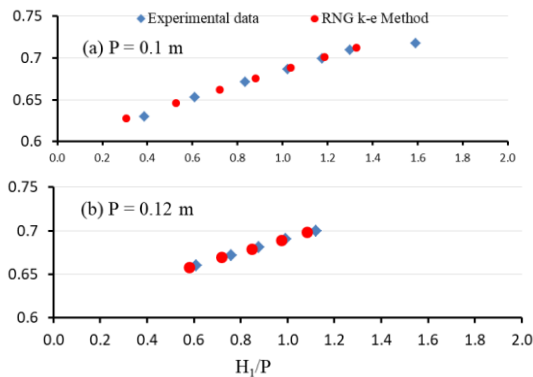


Figure 11. Comparison of numerical and experimental  $C_d$  for different  $H_1/P$ .

### 4.5 Velocity Streamlines

The water entry boundary section was used to produce sample locations of velocity streamlines, which were subsequently dispersed. The main channel domain's streamlines were classified as surface, intermediate, or bed lines, depending on their depth below the channel's surface. Each of the 25 velocity streamlines of the flow shown in Figure 12 was created so that its dividing points could be analyzed. Straight lines travel upstream from the main channel, over the crested weir, and onward toward the downstream exit of the main river through a curved descent.

Figure 13, show that the velocity streamlines along the bed curved dramatically to go around the weir, which was another interesting thing to see. This phenomenon may be useful for determining how deposited sediments in real rivers affect bed level and corresponding water

level during flood seasons, as the streamlines contacting the weir wall cause the return flow due to recirculation of streamlines. On the other hand, passing the steep crested weir, the streamlines at the free surface edge were seen to have a rather smooth curvature. The streamlines were quite far from the weir wall in the downstream part, creating a pocket of air.

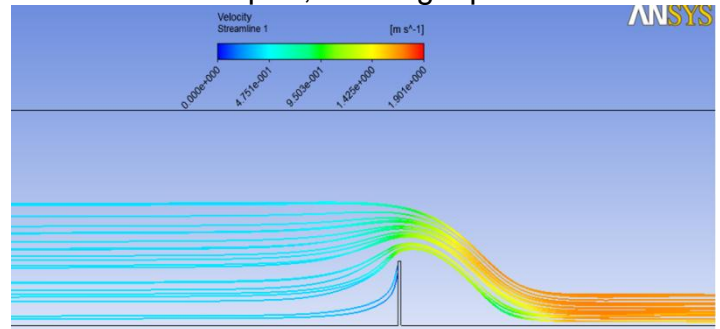


Figure 12. Streamline layout above weir for  $Q= 21$  L/s and  $P=0.12$  m.

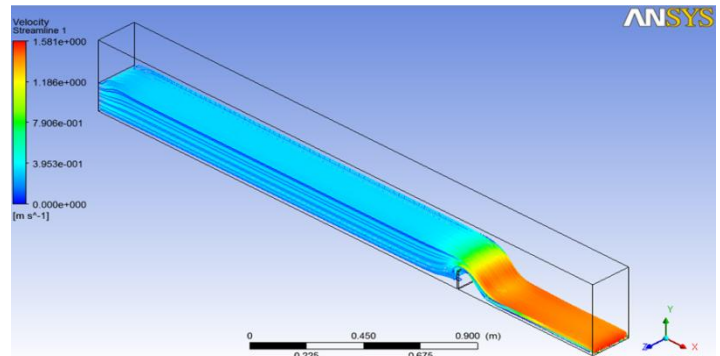


Figure 13. Face centre of streamlines above weir for  $Q = 12$  L/s and  $P= 0.1$  m.

## 5. CONCLUSIONS

In the present study, both experimental and numerical approach used for the investigation of rectangular sharp crested weirs. As indicated earlier, experiments are made with a 20 cm width of channel and full width rectangular weir for two different weir heights. According to the results of this study the conclusions was summarized to the following points:

1. A higher ratio of  $H_1/P$  resulted in a higher discharge coefficient  $C_d$ .
2. When comparing several models for solving flow in a channel passed over a steep crested weir, the RNG k-epsilon model has the lowest average percentage of error.
3. The variations in mass between the channel's entrance and its outflow were one of the factors used to evaluate its convergence. Its equilibrium

state should produce a negligible contribution to the entire net flow.

4. The numerical approach was used to compute the flow properties across the sharp crested weir, and the residual was reduced to  $1 \times 10^{-5}$  while maintaining a highly accurate mass balance between the intake and outlet.

### Funding

These studies have not been supported financially.

### Conflict of interest

The authors declare that the research was conducted in the absence of any commercial or financial relationships that could be construed as a potential conflict of interest.

### References

- Sargison, J.E. and Percy, A., 2009. Hydraulics of broad-crested weirs with varying side slopes. *Journal of irrigation and drainage engineering*, 135(1), pp.115-118.
- Desai, R. and Patil, L. (2015). "Performance Comparison of Various Labyrinth Side Weirs' ", *International Journal of Application or Innovation in Engineering & Management (IJAEM)*, 4 (6), p.68-73.
- Hadi A., Navid O. (2013), "Sharp-Crested Weir Discharge Coefficient; *Journal of Civil Engineering and Urbanism*. 3, Issue 3: 87-91 (2013)
- Hossein A. and Seyed H. (2013), "Experimental and 3-D Numerical Simulation of Flow over a Rectangular Broad- Crested Weir" *International Journal of Engineering and Advanced Technology (IJEAT)* ISSN: 2249 – 8958, Volume-2, Issue-6.
- Mahmoud R. and Mohammad T. (2015), "Numerical Modeling of Sharp-Crested Triangular Plan Form Weirs Using FLUENT" *Indian Journal of Science and Technology*, 8(34), DOI: 10.17485/ijst/2015/v8i34/78200,
- Mahtabi, G. and Arvanaghi, H., 2018. Experimental and numerical analysis of flow over a rectangular full-width sharp-crested weir. *Water Science and Engineering*, 11(1), pp.75-80.
- Hamid and Rasoul (2020), "Three dimensional flow simulation over a sharp-crested V-Notch weir" *Flow Measurement and Instrumentation*, Volume 71 DOI: 10.1016/j.flowmeasinst.2019.101684, 101684
- Ramamurthy R. Tadayon Z. (2009) "Numerical simulation of sharp-crested weir flow" *canadian Journal of Civil Engineering* 36(9):1530-1534.
- Zaid, P.O., 2022. Hydraulic Performance of Moderate Stepped Spillway using ANSYS-FLUENT Software (Master thesis, Salahaddin University-Erbil).
- Zaid, P.O. and Abo, A.A., (2023). Determination the Location of an Air Inception Point for Different Configurations of Stepped Spillways using CFD.
- Malekzadeh, F., Salmasi, F., Abraham, J. and Arvanaghi, H., 2022. Numerical investigation of the effect of geometric parameters on discharge coefficients for broad-crested weirs with sloped upstream and downstream faces. *Applied Water Science*, 12(5), p.110.
- Singh, P. and Sen, D., 2023. Flow-Through Short-Crested Trapezoidal Weirs: Effect of Downstream Slope. *Journal of Irrigation and Drainage Engineering*, 149(8), p.06023002.